



Tertiary treatment of urban wastewater by solar and UV-C driven advanced oxidation with peracetic acid: Effect on contaminants of emerging concern and antibiotic resistance

Luigi Rizzo^{a,*}, Teresa Agovino^a, Samira Nahim-Granados^b, María Castro-Alfárez^b,
Pilar Fernández-Ibáñez^{b,c}, María Inmaculada Polo-López^{b,**}

^a Department of Civil Engineering, University of Salerno, Via Giovanni Paolo II 132, 84084, Fisciano, SA, Italy

^b CIEMAT-Plataforma Solar de Almería, P.O. Box 22, Tabernas, Almería, Spain

^c Nanotechnology and Integrated BioEngineering Centre, School of Engineering, University of Ulster, Newtownabbey, Northern Ireland, United Kingdom

ARTICLE INFO

Article history:

Received 4 September 2018

Received in revised form

8 November 2018

Accepted 12 November 2018

Available online 14 November 2018

Keywords:

Advanced oxidation processes

Antibiotic-resistant bacteria

Peracetic acid

Solar driven processes

Wastewater treatment

Water disinfection

ABSTRACT

Photo-driven advanced oxidation process (AOP) with peracetic acid (PAA) has been poorly investigated in water and wastewater treatment so far. In the present work its possible use as tertiary treatment of urban wastewater to effectively minimize the release into the environment of contaminants of emerging concern (CECs) and antibiotic-resistant bacteria was investigated. Different initial PAA concentrations, two light sources (sunlight and UV-C) and two different water matrices (groundwater (GW) and wastewater (WW)) were studied. Low PAA doses were found to be effective in the inactivation of antibiotic resistant *Escherichia coli* (AR *E. coli*) in GW, with the UV-C process being faster (limit of detection (LOD) achieved for a cumulative energy (Q_{UV}) of 0.3 kJ L^{-1} with $0.2 \text{ mg PAA L}^{-1}$) than solar driven one (LOD achieved at $Q_{UV} = 4.4 \text{ kJ L}^{-1}$ with $0.2 \text{ mg PAA L}^{-1}$). Really fast inactivation rates of indigenous AR *E. coli* were also observed in WW. Higher Q_{UV} and PAA initial doses were necessary to effectively remove the three target CECs (carbamazepine (CBZ), diclofenac and sulfamethoxazole), with CBZ being the more refractory one. In conclusion, photo-driven AOP with PAA can be effectively used as tertiary treatment of urban wastewater but initial PAA dose should be optimized to find the best compromise between target bacteria inactivation and CECs removal as well as to prevent scavenging effect of PAA on hydroxyl radicals because of high PAA concentration.

© 2018 Elsevier Ltd. All rights reserved.

1. Introduction

The concern for the release into the environment of micro-contaminants from point sources, such as wastewater treatment plants (Petrie et al., 2015), as well as the need of wastewater reuse, due to the lack of fresh water sources (Fatta Kassinos, 2015), have been stimulating the discussion in the last years about new relevant regulations (JRC, 2015; Brack et al., 2017) to make urban wastewater treatment plants (UWTPs) effluents safer. As matter of fact, because of inconsistent national legislation across Member States, the European Commission is working on a legislative proposal on minimum quality requirements (MQR) for water reuse in agricultural

irrigation and aquifer recharge (Rizzo et al., 2018). Meanwhile, in the attempt to minimize the release of micro-contaminants (also known as contaminants of emerging concern, CECs) from UWTPs in the environment, Switzerland enacted a regulation entered into force on January 2016, which requires the upgrade of UWTPs within the next twenty years (www.bafu.admin.ch). Accordingly, a selection of CECs from a list of twelve compounds need to be removed from the effluent by 80% (Bourgin et al., 2018). The increasing interest toward CECs and other emerging contaminants, such as antibiotic-resistant bacteria (ARB) and genes (ARGs), as well as the ongoing discussion on new related regulations, have driven the attention on UWTPs that are not or poorly effective to successfully address these new challenges (Rizzo et al., 2013; Petrie et al., 2015; Krzeminski et al., 2019). In a multi-barrier approach, typically implemented in UWTPs trains, the most important role to minimize the release of CECs and the risk of antibiotic resistance spread into the environment relies on tertiary treatment (Ferro

* Corresponding author.

** Corresponding author.

E-mail addresses: l.rizzo@unisa.it (L. Rizzo), mpolo@psa.es (M.I. Polo-López).

et al., 2015; Bourgin et al., 2018). Unfortunately, consolidated tertiary treatments either did not show to be effective or did result in some drawbacks. As matter of fact, chlorination, typically used as disinfection step before UWTP effluent disposal or reuse, is poorly effective in the removal of CECs (Fu et al., 2018) and in controlling antibiotic resistance (Fiorentino et al., 2015; Yuan et al., 2015), as well as results in the formation of hazardous disinfection by-products (DBPs) (Huang et al., 2016; Keun-Young et al., 2016). UV-C disinfection is effective in the inactivation of pathogens when sand filtration is used as pre-treatment, but poor or not effective at all (depending on the characteristics of the target molecule) in the removal of CECs (Lian et al., 2015). Tertiary treatment by ozonation can inactivate pathogens and remove CECs, but an additional post-treatment step can be necessary to remove ozonation by-products (i.e., nitrosodimethylamine and bromate) (Hollender et al., 2009). Activated carbon adsorption is also an effective tertiary treatment for the removal of CECs (Rizzo et al., 2015; Ahmed, 2017) but an additional disinfection process may be necessary, in particular to meet more stringent standards for wastewater reuse. Due to their efficiency in the removal of CECs and inactivation of pathogens because of the formation of reactive oxygen species (ROS), such as hydroxyl radicals (HO^\bullet), advanced oxidation processes (AOPs) represent a possible alternative to conventional tertiary treatments. AOPs can be classified in different ways, one being photo (among which UV/ H_2O_2 , photo-Fenton and TiO_2 photocatalysis) and not photo (such as Fenton, O_3 , $\text{O}_3/\text{H}_2\text{O}_2$ etc.) driven AOPs. Photo-driven AOPs, can be also operated with solar radiation to save energy costs (Malato et al., 2009). Homogeneous photo-driven AOPs (such as UV/ H_2O_2 and photo-Fenton) are more attractive than heterogeneous photocatalytic processes (such as UV/ TiO_2) for short term application as tertiary treatment method of urban wastewater. As matter of fact, the technology of heterogeneous processes is not yet fully mature for large scale applications, basically for limitations related either to catalyst removal after treatment or fixing catalyst on a support (Sacco et al., 2018), and it would be more expensive than homogeneous photo-driven AOPs based technology. Peracetic acid (PAA) is increasingly used as an alternative option to chlorination in wastewater disinfection (Antonelli et al., 2013; Formisano et al., 2016). However, disinfection efficiency (Formisano et al., 2016) and CECs removal (Cai et al., 2017) may be improved by coupling PAA with UV radiation, due to the formation of HO^\bullet . Accordingly, the possible use of this process as homogeneous photo-driven AOP for tertiary treatment of urban wastewater is worthy of investigation. In particular, before any possible up-scale it would be of interest to examine the process efficiency in the removal of CECs at environmentally significant concentrations as well as its effect on antibiotic resistance. Therefore, in the present work, UV/PAA process at pilot scale was investigated for the first time in the inactivation of an antibiotic resistant (AR) (sulfamethoxazole) *Escherichia coli* (*E. coli*) strain, and in the degradation of a mixture of three CECs: (anticonvulsant) Carbamazepine (CBZ), (analgesic) Diclofenac (DCF) and (antibiotic) Sulfamethoxazole (SMX), at initial concentration of $100 \mu\text{g L}^{-1}$ each, in a lower complexity aqueous matrix (namely groundwater (GW)). Subsequently, UV/PAA process was investigated on secondary treated wastewater (WW) samples to evaluate the inactivation of indigenous AR *E. coli* and the degradation of the same mixture of CECs. The effect of light source (solar light Vs UV-C radiation) was also investigated in both aqueous matrices (GW and WW). *E. coli* was chosen as model microorganism because it is considered among the most important vectors in the dissemination of antimicrobial resistance in the environment (Rizzo et al., 2013) as well as because it is used as pathogen indicator in regulations and guide lines for wastewater disposal and reuse (USEPA, 2012; ISO, 2015). CBZ, DCF and SMX were selected as model CECs because they are typically

detected in urban wastewater (Petrie et al., 2015).

2. Material and methods

2.1. Chemicals

Carbamazepine (CBZ), Diclofenac (DCF) and Sulfamethoxazole (SMX), all high purity grade (>99%), were purchased from Sigma-Aldrich. Peracetic Acid (PAA) solution, containing 30% w/w of PAA and 4.5% w/w of H_2O_2 was purchased from Sigma-Aldrich and used as obtained. Sodium thiosulfate ($\text{Na}_2\text{S}_2\text{O}_3$, 99% w/w) and bovin liver catalase were used, as received from Sigma-Aldrich. Titanium IV oxysulfate (Riedel-de-Haën, Germany) was used, as obtained from the manufacturer.

2.2. Water matrices

To evaluate water matrix effect on UV/PAA process tests were performed with both GW and WW. GW was collected from a borehole located on the Plataforma Solar de Almeria (PSA) site with depth of approximately 200 m. Physical-chemical characteristics of both water matrices are given in Table 1.

GW samples were inoculated with SMX resistant *E. coli* strain selected from the effluent of the biological process (activated sludge) of Almeria (Spain) UWTP, according to the procedure explained in the subsequent paragraph 2.4. WW samples were also taken after biological process (just upstream of disinfection unit) from the same UWTP during spring-summer time (June–August 2017), and used for disinfection/oxidation experiments without inoculum. Samples were collected in amber glass bottles and stored at 4°C for a maximum of two days.

2.3. AOPs and control experiments

The experimental design included two pilot scale reactors, namely a Compound Parabolic Collector (CPC) for outdoor sunlight experiments and a UV-C reactor (UV-C).

2.3.1. Sunlight/PAA experiments with CPC

The CPC reactor used was previously described (Polo-López et al., 2010). Briefly, it consists of two 60 L tube modules, each one equipped with 10 cylindrical glass tubes made of borosilicate glass, with a diameter of 5 cm, a length of 150 cm and a thickness of 2.5 mm, to allow a 90% transmission of UVA in the natural solar spectrum. The photoreactor is tilted at 37° with respect to the horizontal to maximize solar radiation. A tank housed in the lower

Table 1
Characteristics of GW and WW samples.

Parameters	GW	WW
	Av \pm SD	Av \pm SD
Cl^- (mg L^{-1})	337.1 \pm 76.7	341.3 \pm 16.3
NO_3^- (mg L^{-1})	12.1 \pm 1.2	23.4 \pm 5.3
SO_4^{2-} (mg L^{-1})	200.9 \pm 39.6	84.3 \pm 7.7
NH_4^+ (mg L^{-1})	–	23.6 \pm 24.2
Na^+ (mg L^{-1})	517.8 \pm 94.1	197.5 \pm 2.8
Mg^{2+} (mg L^{-1})	67.2 \pm 15.4	31.4 \pm 6.9
K^+ (mg L^{-1})	8.87 \pm 1.7	27.1 \pm 0.8
Ca^{2+} (mg L^{-1})	71.6 \pm 16.8	71.4 \pm 11.8
pH	8.2 \pm 0.5	7.5 \pm 0.1
Conductivity ($\mu\text{S cm}^{-1}$)	2396.0 \pm 0.10	1921.0 \pm 21.4
Turbidity (NTU)	0.6 \pm 0.1	6.3 \pm 4.4
TOC (mg L^{-1})	1.80 \pm 1.6	24 \pm 1.0
IC (mg L^{-1})	170.2 \pm 9.3	38 \pm 8.1
AR <i>E. coli</i> (CFU mL^{-1})	–	1337 \pm 5663

part of the pilot plant is connected to a pump, which allowed to operate the modules in a recirculation mode. The CPC reactor has a total illuminated volume of 45 L and it was operated with a water flow rate of 30 Lmin⁻¹. This flow rate guarantees a turbulent regime, which results in a proper homogenization of water samples and in a good contact between bacteria, contaminants and oxidant. Disinfection experiments were carried out during 300 min of solar exposure on clear sunny days at PSA from May 2017 to August 2017. More specifically, firstly the solar photoreactor was filled in with 60 L of water matrix (GW or RW) and then, the mixture of the three CECs (100 µg L⁻¹ of initial concentration each) and the sulfamethoxazole resistant *E. coli* solution (10⁶ CFU mL⁻¹ initial bacterial density) were spiked in. After 5 min of homogenization with the CPC still covered, a control sample was taken in order to ensure the presence of bacteria and contaminants. Then, PAA (initial concentration in the range 0.075–20 mg L⁻¹) was added to the reactor tank and after 10 min of recirculation, the experiment started as the cover was removed. Samples were collected at regular intervals depending on the treatment. Water temperature ranged from 21.0 to 47.7 °C and pH ranged from 8.04 to 9.41. A fixed pyranometer (Model CUV5, 280–400 nm, Kipp & Zonen, Netherlands) registered in continuous mode the incident light. The inactivation and degradation rates were plotted as a function of both the experimental time (t) and the cumulative energy per unit of volume (Q_{UV}) received in the photoreactor, commonly used to compare results under different conditions (Malato et al., 2009), and calculated by Equation (1):

$$Q_{UV,n} = Q_{UV,n-1} + \Delta t_n \cdot UV_{G,n} \cdot A_r / V_t \quad \Delta t_n = t_n - t_{n-1} \quad (1)$$

where Q_{UV,n} and Q_{UV,n-1} are the UV energy accumulated per liter (kJ L⁻¹) at times n and n-1, UV_{G,n} is the average incident radiation on the irradiated area, Δt_n is the experimental time of sample, A_r is the illuminated area of the reactor (m²) and V_t is the total volume of water treated (L). Each experiment was performed in duplicate, between 10 a.m. and 16 p.m. local time, and the results were plotted as the average of the two replicates.

2.3.2. UV-C plant

The UV-C reactor is a plant equipped with three UV-C lamps (254 nm peak wavelengths, 230 W) connected in series, with a flexible configuration that allow the system to operate with a single lamp, two or three lamps in recirculating batch mode or continuous flow mode. In this study, only one lamp was used and the illuminated volume was 4.17 L, which corresponds to a total volume in the plant of 80 L. Disinfection/oxidation experiments were carried out during 180 min at PSA from May 2017 to August 2017. More specifically, firstly the reactor was filled in with water matrix (GW or WW) and then, the mixture of the three CECs (100 µg L⁻¹) and the sulfamethoxazole resistant *E. coli* solution (10⁶ CFU mL⁻¹) were spiked in. After 15 min of homogenization, with the lamp still switched off, initial sample was taken in order to ensure the presence of bacteria and contaminants. Then, PAA (initial concentration in the range 0.075–20 mg L⁻¹) was added to the reactor tank and after 15 min of recirculation, the experiment started and the lamp was switched on. Samples were collected at regular intervals depending on the treatment. A fixed controller (ProMinent) housed in the back of the reactor, monitored in continuous water flow rate (46 Lmin⁻¹) and UV-C lamp intensity (33.7 Wm⁻² for WW and 99.7 Wm⁻² for GW). The equipment registers, in continuous during the test, the sensor measurements in terms of incident irradiation (Wm⁻²), which is the UV-C radiation energy rate incident on a surface per unit area. The accumulated energy rate was calculated according to Eq. (2):

$$Q_{UV,C} \text{ (KJ L}^{-1}\text{)} = \text{Dose (Jm}^{-2}\text{)} \cdot A_i / V_T \text{ (m}^2\text{L}^{-1}\text{)} \text{ (KJ(1000 J)}^{-1}\text{)} \quad (2)$$

where Q_{UV,C} is the accumulated UV-C energy per L, Dose is the UV-C ultraviolet irradiation (Wm⁻²) emitted by the lamp multiplied by the illumination time, A_i (0.28 m²) is the irradiated surface, V_T (80 L) is the total volume of the water into the pilot plant and V_i (4.17 L) is the total irradiated volume. Each experiment was performed in duplicate and the results were plotted as the average of the two replicates.

2.4. Selection of antibiotic resistant *E. coli* strain

The antibiotic resistant *E. coli* strain inoculated in GW for disinfection experiments was isolated from the effluent of the biological process (activated sludge) of Almeria UWTP by membrane filtration method and subsequent cultivation on selective medium, according to a previously published procedure (Rizzo et al., 2014). More specifically, 50 mL of wastewater and its serial dilutions were filtered through sterile membranes (cellulose nitrate, 0.45-µm pore size, 47 mm diameter, Millipore) which were incubated (24 h, 37 °C) on AR m-FC (Difco) culture medium supplemented with 64 mg L⁻¹ of sulfamethoxazole. Antibiotic concentration was chosen according to the double of the respective minimum inhibitory concentration (MIC) values available in EUCAST database (2014). Some colonies were randomly picked up and frozen at -5 °C using sterile vials of cryobeads (Deltalab). To recover the stock, the vial was slowly unfreezed up to reach room temperature (25 °C). One bead was streaked onto a Petri dish of AR m-FC agar and incubated for 20 h at 37 °C to obtain isolated bacteria colonies. This dish was stored during 1 week in the refrigerator to prepare a fresh *E. coli* culture to make it available for GW disinfection/oxidation experiments. Fresh liquid cultures were prepared taking one colony from the refrigerated stock in the Petri dish using a loop, transferred into 14 mL of liquid LB broth and incubated in a rotary shaker at 100 rpm, during 18–20 h at 37 °C to get the bacterial stationary phase concentration (10⁹ CFU mL⁻¹). Bacterial suspensions were harvested by centrifugation at 3000 rpm for 10 min. Then, the pellet was re-suspended in Phosphate Buffer Saline (PBS) solution and diluted directly into the GW sample for each experiment to reach the initial concentration of 10⁶ CFU mL⁻¹.

2.5. Analytical measurements

Before performing each experiment, water samples were characterized in terms of temperature, pH, conductivity, DOC, inorganic carbon (IC), total carbon (TC), anions and cations. Temperature and pH were measured using a multi parametric sensor WTW multi720. Conductivity was measured by a conductivity meter GLP31 CRISON. Turbidity was measured by a turbidity meter 2100AN model (Hach). DOC, IC and TC were analyzed using a Shimadzu TOC-V-CSN and an auto-sampler ASI-V. DOC was estimated as the difference between the TC and the IC values. Samples were filtered with a 0.22 mm nylon filter (Aisimo, Millipore Millex® GN) before their injection into the equipment. The calibration was performed periodically with potassium hydrogen phthalate in Milli-Q water for TC and a sodium carbonate/sodium bicarbonate (1:1) for IC. Anions and cations were analyzed using ion chromatography, 850 Professional IC – Cation coupled to Metrohm 872 Extension Module. Samples were filtered with a 0.22 mm nylon filter (Aisimo) before injection into the equipment. The calibration was checked before samples measurements by standard solutions of 10 mg L⁻¹ of each anion and cation analyzed. CECs concentrations were monitored by ultra-performance liquid chromatography UPLC (Agilent Technologies, series 1200) with a UV-DAD detector and a C-18 analytical column. The initial conditions were 95% water

with 25 mM formic acid (A) and 5% ACN (B). A linear gradient progressed from 10% to 0% B in 15 min. Re-equilibration time was 3 min with a flow rate of 1 mL min⁻¹. In order to prepare the vial for the detector, firstly, 4.5 mL of sample were filtered using a 0.22- μ m PTFE filter (Millipore). Then, to remove any adsorbed compounds, the filter was washed with 2.5 mL of ACN mixed with the filtered water sample. The prepared solution was transferred into an amber glass vial, put in the UPLC and analyzed using an injection volume of 100 μ L. Retention time, quantification limit (LOQ), detection limits (LOD) and maximum absorption (I) for the MCs are shown in Table S1 (in supplementary information file).

PAA commercially available solutions also contain a percentage of H₂O₂ (4.5% w/w in the solution used in this work), which will contribute to the formation of HO[•]. Accordingly, H₂O₂ residual concentration was also measured in this work to better support explanation and discussion of the results achieved. In particular, H₂O₂ concentration was measured with a spectrophotometer (PG Instruments Ltd T-60-U) at 410 nm in glass cuvettes with a 1 cm of path length based on the formation of a yellow complex from the reaction of titanium IV oxysulfate with H₂O₂ following DIN 38409 H15. Absorbance was read after 5 min incubation time against a H₂O₂ standard curve linear in the 0.1–100 mgL⁻¹ concentration range.

PAA concentration was measured according to the method from HACH (2014). Briefly, 2.5 mL of sample was mixed with 15 mg of N,N-diethyl-p-phenylenediamine (DPD, VWR Chemicals). Absorbance was measured with a spectrophotometer (PG Instruments Ltd T-60-U) at 530 nm after 45 s of incubation time against a PAA standard curve (range 0.05–5 mg L⁻¹).

2.6. Bacterial count

Bacterial count was performed by standard plate counting method through a serial 10-fold dilutions in PBS placed into AR m-FC agar Petri dishes. In particular, when the bacterial load was expected to be high, 50 μ L drop of adequate dilution was plated, instead, when the bacterial load was expected to be low, volume of 500 μ L was spread onto prepared dishes. Antibiotic resistant (AR) *E. coli* colonies were counted after an incubation period of 20 h at 37 °C (limit of detection (LOD) 2 CFU mL⁻¹). Measurements were carried out in duplicates in order to plot average values. The results were highly reproducible and the standard deviation of the replicates is showed in the graphs as error bars. Stock solutions of bovine liver catalase (50 mg L⁻¹) and sodium thiosulfate (100 mg L⁻¹) were freshly prepared every day and added 20 μ L mL⁻¹ and 1 μ L mL⁻¹ respectively to all water samples taken from the reactors in order to remove any residual concentration of PAA and H₂O₂.

3. Results

3.1. Inactivation of AR *E. coli* by sunlight/PAA in CPC

3.1.1. Control tests

Control experiments were performed with PAA and sunlight as standalone processes, respectively. The effect of PAA on the inactivation of AR *E. coli* under dark conditions was investigated for three PAA concentrations (0.075, 1 and 2 mg L⁻¹) in GW. The LOD was achieved for 1 and 2 mg PAA L⁻¹, with 4 and 5 log unit inactivation respectively, after 15 min (Fig. 1). The lower investigated dose (0.075 mg PAA L⁻¹) resulted only in half log unit inactivation after 180 min, possibly due to the low initial concentration of both PAA and H₂O₂ (0.039 mg L⁻¹). The LOD was even achieved for sunlight experiment, but after 300 min treatment (53.67 kJ L⁻¹).

Part of PAA initial concentration was consumed as the oxidant

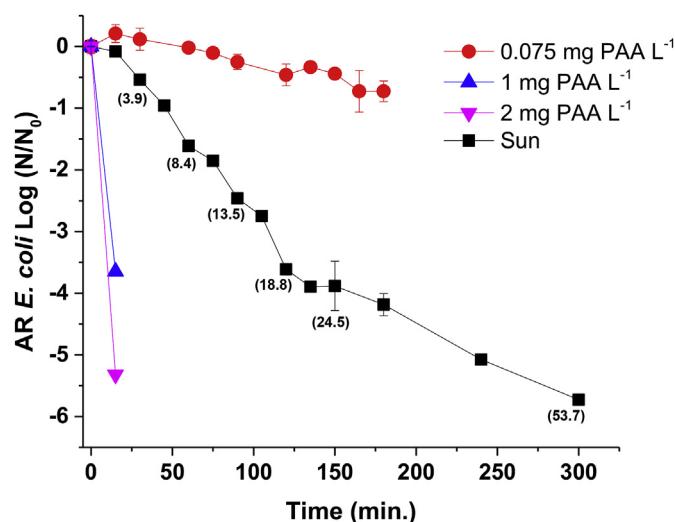


Fig. 1. Inactivation of AR *E. coli*: control tests in dark with PAA and sunlight as standalone processes. Q_{UV} values are given between brackets.

solution was added to GW sample; as can be observed from Figure S11, PAA concentration measured just after the addition of PAA solution ($t = 0$) is lower than the corresponding initial concentration dosed. Moreover, PAA was almost totally consumed after 300 min treatment when 1 mg PAA L⁻¹ was added; while only 50% was consumed when initial PAA was 2 mg PAA L⁻¹.

3.1.2. Effect of PAA initial concentration

Since AR *E. coli* inactivation was quite fast between 1 and 2 mg PAA L⁻¹ under dark conditions, lower PAA concentrations (in the range 0.075–1.0 mg L⁻¹) were investigated during sunlight/PAA tests. Q_{UV} and solar exposure time required to reach the LOD for the inactivation of AR *E. coli*, decreased as PAA dose was increased. More specifically, in GW the best performance was achieved after 30 min with 0.2 mg PAA L⁻¹ ($Q_{UV} = 4.40$ kJ L⁻¹) (Fig. 2a). Inactivation rates were faster compared to sunlight experiment where LOD was achieved after 300 min treatment with a higher energy requirement (53.67 kJ L⁻¹).

Moreover, the lower investigated PAA initial concentration (0.075 mg L⁻¹) did not produce a sufficient amount of hydroxyl radicals to improve AR *E. coli* inactivation compared to solar radiation as standalone process. PAA was almost totally consumed during treatment process (Figure S12a) and a fluctuation in residual H₂O₂ concentration (1 mg PAA L⁻¹ solution) was observed (Figure S12b).

The effect of sunlight/PAA process was also investigated in WW (Fig. 2b). WW was not inoculated with the selected AR *E. coli* strain, therefore the inactivation curves refer to the indigenous *E. coli* population resistant to SMX (initial bacterial density 70–7000 CFU mL⁻¹). In particular, different initial PAA concentrations (1, 2, 4 and 10 mg L⁻¹) were investigated and the best performance was observed for 10 mg PAA L⁻¹ being the LOD achieved after 2 min irradiation ($Q_{UV} = 0.28$ kJ L⁻¹) (Fig. 2b). The LOD was achieved for all the investigated conditions, being the sunlight process the slower ($Q_{UV} = 38.03$ kJ L⁻¹ after 210 min). In agreement with the results observed in GW experiments, PAA was almost totally consumed during treatment process in WW, for PAA initial concentrations in the range 1–10 mg L⁻¹, and only when a higher dose (20 mg L⁻¹) was investigated (to evaluate possible effect on CECs degradation) a residual was detected (Figure S13a). Fluctuation in residual H₂O₂ concentration (1 mg PAA L⁻¹ solution) was also observed in WW experiments (Figure S13b).

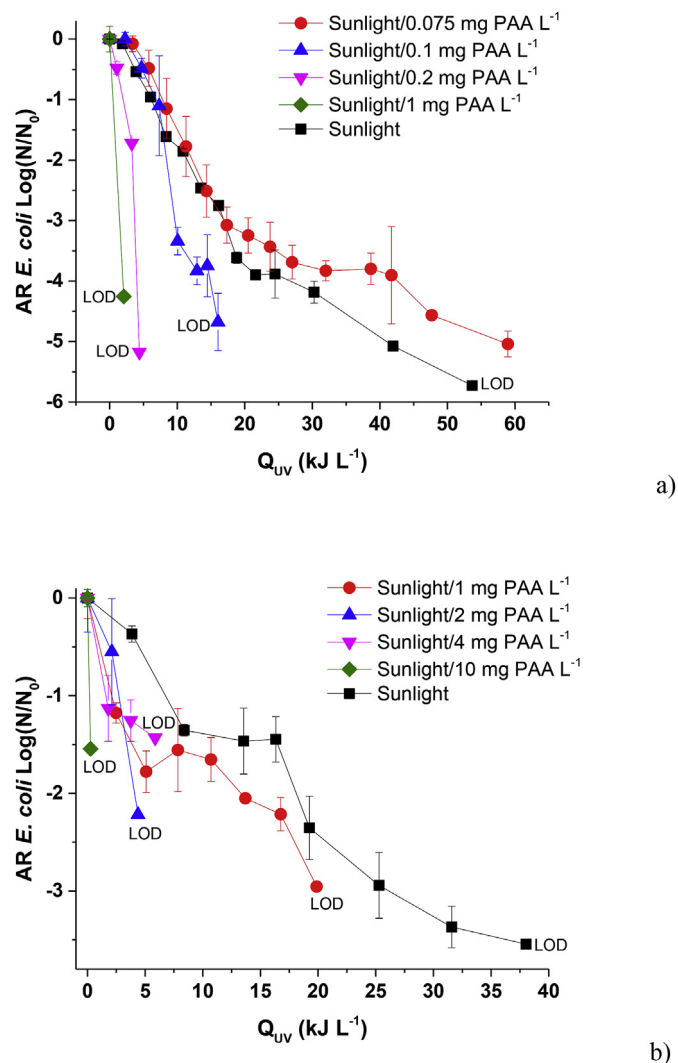


Fig. 2. Inactivation of AR *E. coli* by sunlight/PAA in CPC: effect of initial PAA concentration in GW (a) and WW (b).

3.2. Degradation of CECs by sunlight/PAA in CPC

Typically, when AOPs are investigated in the removal of pollutants from water, an effect of water matrix composition can be observed, with a decreased process efficiency as the complexity of the aqueous matrix increases (e.g., from deionized water solutions to GW and WW). The decreased efficiency can be typically explained by the occurrence of readily oxidized molecules (also known as oxidant demand of the target water matrix) in more complex water matrices compared to less complex ones. Actually, this behaviour was not evident in the removal of CBZ and DCF by sunlight/PAA, while it was evident for SMX, as explained in the subsequent paragraphs.

3.2.1. Control tests

Control experiments to evaluate the effect of PAA and sunlight as standalone processes, on the target CECs were also carried out. In particular, the effect of PAA dose in darkness was investigated at 2 mg L⁻¹ initial concentrations (Fig. 3).

Unlike of CBZ, DCF was effectively oxidized by PAA after 60 min (80% removal), while SMX was removed at a lower rate (52% after 300 min) compared to DCF. Photodegradation rate by sunlight as

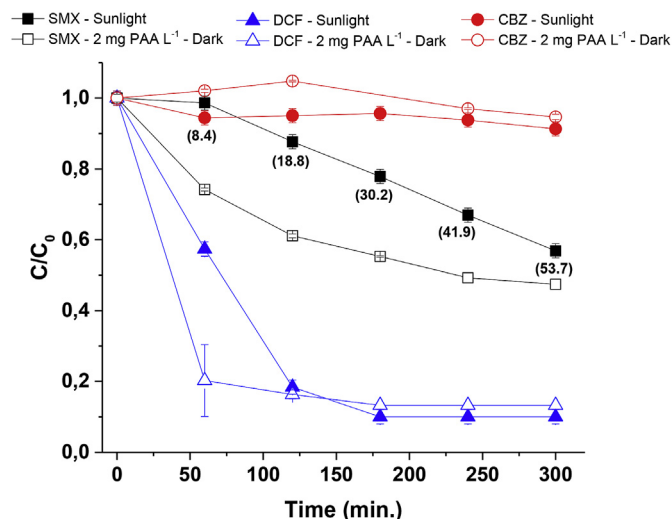


Fig. 3. Degradation of CECs: control tests with PAA and sunlight as standalone processes.

standalone process changed depending on the target CEC: from no degradation for CBZ, to moderate degradation for SMX (43% after 300 min irradiation and 53.7 kJ L⁻¹), to high degradation for DCF (90% after 180 min and 30.2 kJ L⁻¹).

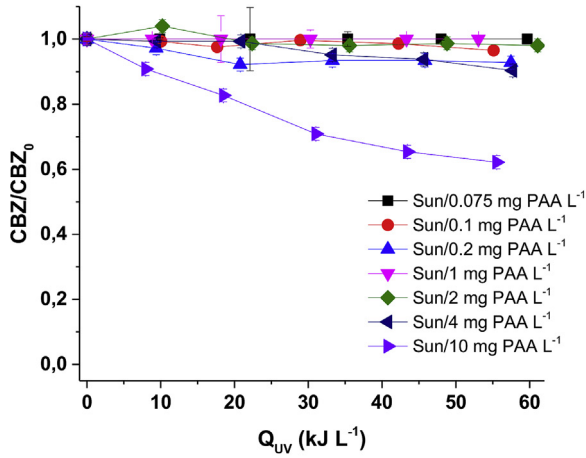
3.2.2. Effect of PAA initial concentration

The effect of sunlight/PAA process on CECs was investigated for both water matrices (GW and WW). CBZ was refractory to sunlight/PAA process too. Only when initial PAA concentration was increased to 10 mg L⁻¹ a significant degradation (40%) was observed after 300 min treatment (Q_{UV} = 55.53 kJ L⁻¹) in GW (Fig. 4a).

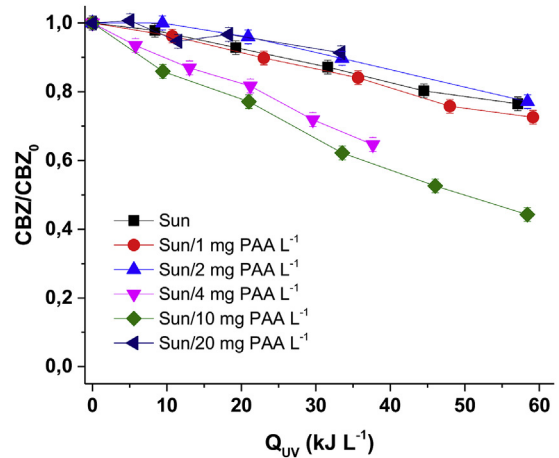
Even for DCF, sunlight/PAA process enhanced degradation compared to PAA as standalone process in GW matrix. The best performance was observed with 2 mg PAA L⁻¹ that allowed to reach the quantification limit (QL) at Q_{UV} = 10.23 kJ L⁻¹ (Fig. 4b). Interestingly, as PAA concentration was further increased from 4 to 10 mg L⁻¹, DCF degradation rate decreased. Similar behaviour was observed for SMX (Fig. 4c). SMX degradation increased as PAA dose was increased from the lower dose (0.075 mg L⁻¹) to 4 mg L⁻¹ (the QL was reached after 60 min and Q_{UV} = 9.49 kJ L⁻¹) then started to decrease, although to a lower rate compared to DCF.

Due to the higher oxidant demand of WW, PAA doses lower than 1.0 mg L⁻¹ were not investigated and 20 mg PAA L⁻¹ was added (Fig. 5). The behaviour of sunlight/PAA process in WW matrix was quite different compared to GW. As matter of fact, a moderate efficiency in CBZ degradation was also observed at lower PAA doses; for example 2 mg PAA L⁻¹ resulted in 23% CBZ degradation after 300 min (Q_{UV} = 58.39 kJ L⁻¹) and process efficiency increased as initial PAA concentration was increased to 4 and 10 mg L⁻¹, being the best removal (56%) observed with 10 mg PAA L⁻¹ after 300 min (Q_{UV} = 58.39 kJ L⁻¹) (Fig. 5a). But as PAA was further increased (20 mg L⁻¹), process efficiency drastically decreased, thus showing a similar behaviour to DCF and SMX in GW experiments.

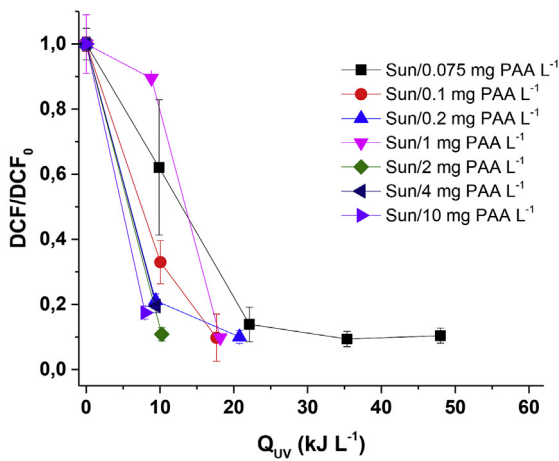
DCF degradation was drastically affected by aqueous matrix. The best performance in WW was observed with 20 mg PAA L⁻¹ that reached the QL after 120 min (Q_{UV} = 11.46 kJ L⁻¹) (Fig. 5b). Moreover, aqueous matrix significantly affected process efficiency at lower PAA concentrations; for example, only 32% degradation was achieved with 2 mg L⁻¹ of PAA in WW, compared to 99% observed in GW after 60 min treatment (Q_{UV} = 10.23 kJ L⁻¹). Similarly to the results observed for GW, SMX degradation by sunlight/PAA



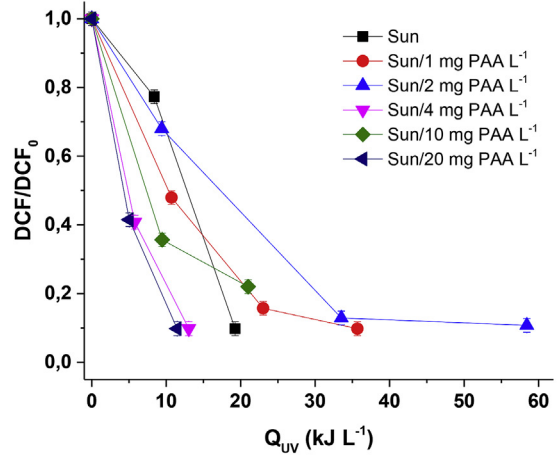
a)



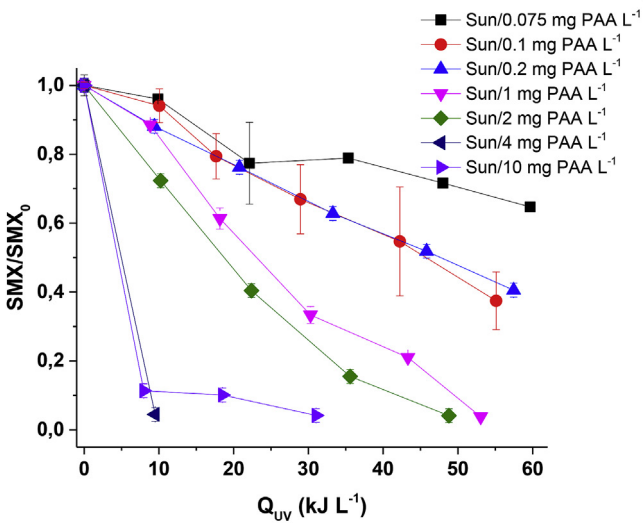
a)



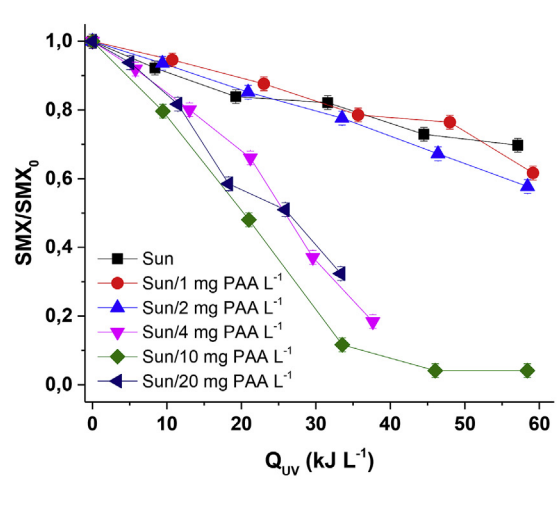
b)



b)



c)



c)

Fig. 4. Effect of sunlight/PAA process on CECs in GW: CBZ (a), DCF (b) and SMX (c).

Fig. 5. Effect of sunlight/PAA process on CECs in WW: CBZ (a), DCF (b) and SMX (c).

increased as PAA concentration was increased (Fig. 5c). The QL was achieved for 10 mg L⁻¹ of PAA after 240 min ($Q_{UV} = 46.03 \text{ kJ L}^{-1}$). But a further increase of initial PAA dose to 20 mg L⁻¹ resulted in a decreased degradation efficiency, thus confirming the trend already observed in GW experiments.

3.3. Inactivation of AR *E. coli* by UV-C/PAA process

Really fast inactivation rates were observed in GW for UV-C/PAA process compared to sunlight/PAA (Fig. 6). The LOD was achieved for all PAA investigated doses and even for UV-C as standalone process. In particular, total inactivation was achieved in a few minutes for 0.15 mg PAA L⁻¹ (2 min) and 0.2 mg PAA L⁻¹ (4 min).

With 0.075 mg L⁻¹ and 0.1 mg L⁻¹ of PAA LOD was reached with

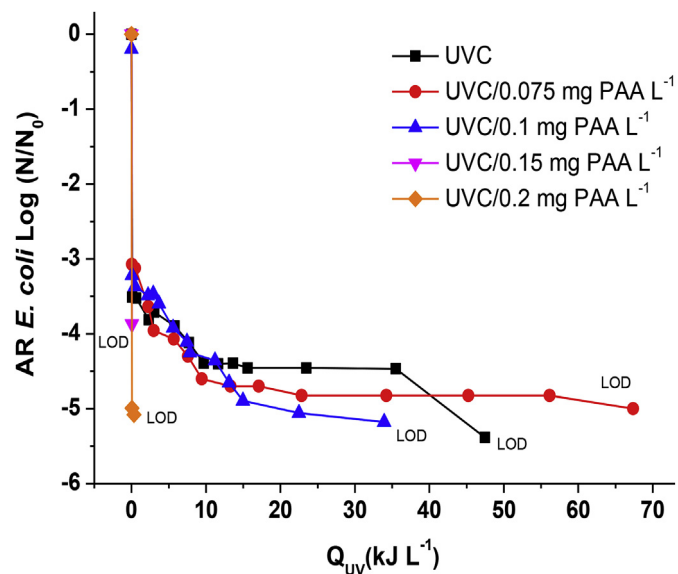


Fig. 6. Inactivation of AR *E. coli* by UV-C/PAA process in GW.

a cumulative energy dose of 67.39 kJ L^{-1} (180 min irradiation) and 33.93 kJ L^{-1} (90 min irradiation), respectively.

Due to both the higher oxidant demand of WW compared to GW and the total consumption of PAA and H_2O_2 in GW experiments, higher concentrations of PAA (4, 10 and 20 mg L^{-1}) were investigated in UV-C/PAA experiments in WW. As matter of fact, the initial AR *E. coli* concentrations were really low ($63, 35$ and 2 CFU mL^{-1} for 4, 10 and 20 mg PAA L^{-1} experiments, respectively) and the LOD was achieved in 2 and 15 min for 10 and 4 mg PAA L^{-1} experiments, respectively (data not shown).

3.4. Degradation of CECs by UV-C/PAA process

The effect of PAA dose on the degradation of the target CECs by UV-C/PAA process was investigated in both water matrices (GW and WW). Among the three CECs, CBZ confirmed its lower degradation. No significant differences were observed between UV-C as standalone process (20% degradation after 180 min treatment and with an energy requirement of 71.78 kJ L^{-1}) and UV-C/PAA process up to $1.0 \text{ mg PAA L}^{-1}$ in GW (Fig. 7a). The best performance (77% removal) was obtained with 10 mg PAA L^{-1} after 150 min and with a Q_{UV} of 71.78 kJ L^{-1} . Residual concentrations of PAA and H_2O_2 are available in supplementary information (Figures S14a and S14b).

For the lower concentration investigated in WW (4 mg PAA L^{-1}) the aqueous matrix effect between GW and WW was not observed (Fig. 7b). But when PAA concentration was increased (10 and 20 mg PAA L^{-1}) the difference between the two matrices increased (e.g., 55% CBZ removal in WW compared to 67% in GW for 10 mg PAA L^{-1} at approximately 21 kJ L^{-1}). Interestingly, at the higher investigated dose (20 mg PAA L^{-1}) the residual concentration of PAA is lower than that one for 10 mg PAA L^{-1} solution, but the corresponding H_2O_2 residual concentration is significantly higher (Figure S15).

The best degradation of DCF in GW was observed for the lower investigated PAA doses ($0.075 \text{ mg PAA L}^{-1}$) compared to sunlight/PAA tests (Fig. 8a). Even in UV-C/PAA tests, process efficiency started to decrease above a certain concentration (1.0 mg L^{-1}) of PAA, being the worst removal observed for the higher investigated PAA dose (10 mg L^{-1}). The water matrix affected the photo-oxidation process, because no drastic efficiency decrease was observed as PAA was increased (Fig. 8b).

SMX was effectively degraded even with UV-C as stand-alone

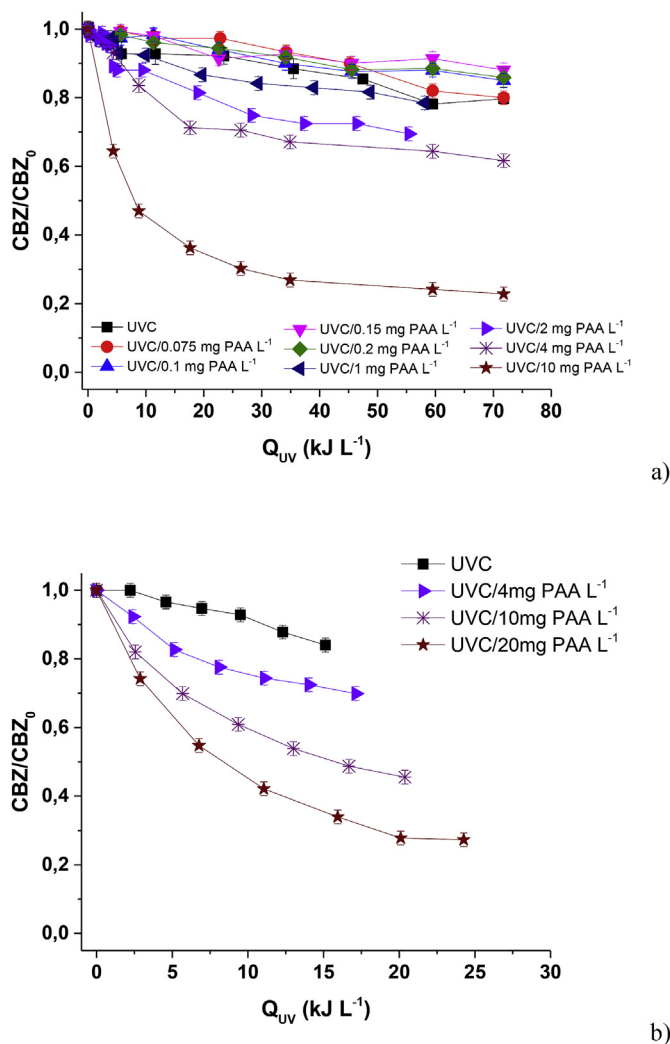


Fig. 7. Effect of UV-C/PAA process on CBZ in GW (a) and WW (b).

process in GW (LOD was achieved with $Q_{\text{UV}} = 5.78 \text{ kJ L}^{-1}$) and WW (LOD observed for $Q_{\text{UV}} < 4.58 \text{ kJ L}^{-1}$), accordingly PAA addition did not significantly improve process efficiency (for 4 mg PAA L^{-1} LOD observed for $Q_{\text{UV}} < 2.4 \text{ kJ L}^{-1}$) (data not shown).

4. Discussion

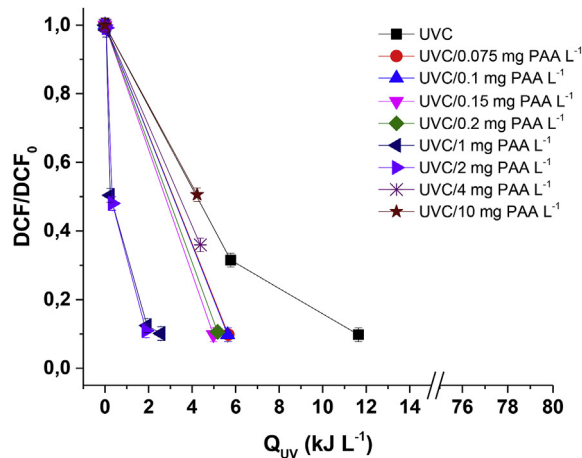
4.1. Photolysis of PAA and effect on PAA and H_2O_2 concentrations

UV/PAA process has been poorly investigated so far, and the previous works have been basically focused on bacteria inactivation (Koivunen and Heinonen-Tanski, 2005; De Souza et al., 2015); only recently its effect on pharmaceuticals has been addressed (Cai et al., 2017). PAA ($\text{CH}_3\text{CO}_3\text{H}$) aqueous solutions commercially available are an equilibrium mixture of acetic acid (CH_3COOH), H_2O_2 , PAA and water, according to the reaction:

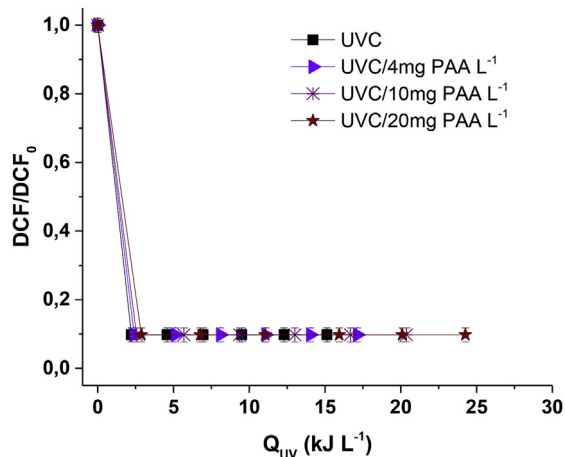


Photolysis of the O–O bond in the PAA molecule results in the formation of HO^\bullet , according to Equation (4) (Caretto and Lubello, 2003):





a)



b)

Fig. 8. Effect of UV-C/PAA process on DCF in GW (a) and WW (b).

The $\text{CH}_3\text{COO}^\bullet$ molecule will rapidly split in CH_3^\bullet and CO_2 (Martin and Gehr, 2007). Moreover, HO^\bullet molecules can also recombine to form H_2O_2 :



The production of PAA (Eq. (3)) and the recombination of HO^\bullet molecules (Eq. (5)) can explain the fluctuations observed in the measurement of residual H_2O_2 (Figure S12b and S13b).

According to the results achieved in this work, the mechanisms of bacterial inactivation and CECs degradation in PAA photolysis are possible related to a combination of effects including photolysis, oxidation (by PAA solution) and formation of HO^\bullet .

4.2. Control tests: effect of radiation and PAA solution on bacteria inactivation and CECs degradation

The effect of sunlight and UV-C radiation on bacteria inactivation is evident from Figs. 2 and 6, respectively. To date, all waterborne pathogenic bacteria, among which *E. coli*, have been found to be amenable to sunlight disinfection (McGuigan et al., 2012). Although the UV-A wavelengths are not sufficiently energetic to alter DNA directly, UV-A play an important role in promoting the formation of intracellular reactive oxygen species (e.g., HO^\bullet) which

can, in turn, damage DNA. UV-C radiation (200–280 nm germicidal wavelength range, peaks at about 260–265 nm) has a direct effect on bacterial cells because it is absorbed by nucleic acids; cell inactivation can take place through UV-induced damages such as the formation of pyrimidine dimers in their DNA (Kowalski, 2009).

While CBZ was not (under sunlight in GW) or poorly (under sunlight in WW and under UV-C radiation) photodegraded, confirming its refractory behaviour to direct photolysis (Calisto et al., 2011), SMX and DCF were significantly degraded under irradiation. DCF has an absorbance peak at 275–280 nm and its degradation under sunlight is the result of two mechanisms: direct photolysis and self-sensitization, being direct photolysis the main one (Zhang et al., 2011). SMX absorbance spectrum is characterized by a peak at 257–268 nm (depending on solution pH) and tails well over 320 nm, which overlap with the solar spectrum (in the 300–325 nm) and make its photodegradation possible (Trovo et al., 2009; Rizzo et al., 2012).

The redox potential of PAA is comparable or even higher than many disinfectants (Zhang et al., 2018), which make it effective in the inactivation of different bacterial populations. Accordingly, our results in terms of AR *E. coli* inactivation under dark conditions (Fig. 1) are consistent with previous results on *E. coli* inactivation (Antonelli et al., 2006). Moreover, the high redox potential can also explain the high oxidation rate of DCF and SMX (Fig. 3).

4.3. Effect of photo-driven AOPs with PAA on bacteria inactivation and CECs degradation

According to Eq. (4), sunlight/PAA and UV-C/PAA processes result in the formation of HO^\bullet species. The role of HO^\bullet in the inactivation of *E. coli* was previously explained through the support of disinfection photocatalytic experiments (Cho et al., 2004). In subsequent studies, a killing mechanism where HO^\bullet progressively damages the cell surface structures leading to the release of intracellular material/molecules was proposed (Foster et al., 2011). Inactivation of microorganisms by photo-driven advanced oxidation with PAA has been mainly investigated by using artificial light while, to our knowledge, only one study was specifically focused on sunlight/PAA process (Formisano et al., 2016) and no previous study evaluated the effect on the inactivation of AR *E. coli*. Formisano et al. (2016) observed a total inactivation of *E. coli* by sunlight/PAA (8 mg PAA L⁻¹) process after 120 min treatment ($Q_{UV} = 7.42 \text{ kJ L}^{-1}$) in WW, with an initial *E. coli* density as high as 10^5 CFU mL^{-1} . These results are different compared to the inactivation rates observed in our work with (i) GW (where the best performance was achieved after 30 min with 0.2 mg PAA L⁻¹ and $Q_{UV} = 4.40 \text{ kJ L}^{-1}$) (Fig. 2a) and (ii) WW (being the best performance and LOD achieved for 10 mg PAA L⁻¹ after 2 min irradiation and $Q_{UV} = 0.28 \text{ kJ L}^{-1}$) (Fig. 2b). The different water matrix and *E. coli* population (total Vs AR *E. coli*) in case (i) and the lower initial bacterial density and the different *E. coli* population in case (ii) may explain the different results observed. Inactivation rates in GW drastically increased when UV-C radiation was used (LOD achieved within 2 min for 0.15 mg PAA L⁻¹ and 4 min with 0.2 mg PAA L⁻¹) instead of sunlight. In WW experiments, the initial AR *E. coli* concentration was really low and the LOD was achieved for all the PAA doses investigated. In a previous work on wastewater disinfection by UV-C/PAA process, *E. coli* inactivation of 3.6 and 4.5 log units were observed for 2 and 4 mg L⁻¹ of PAA, respectively and an UV-C dose as high as UV dose of $120 \text{ mW} \cdot \text{s cm}^{-2}$ (Lubello et al., 2002).

As the effect of photo-driven AOPs with PAA on CECs degradation is of concern, it is worthy to mention that scientific literature is lacking. However, our results are consistent with removal trends of CBZ, DCF and SMX observed in solar driven AOPs (namely photo-Fenton) (Klamerth et al., 2010; Ferro et al., 2015). In our work CBZ

was found to be refractory to sunlight/PAA process, according to the results available in the literature for other solar driven AOPs. For example, only 36.9% degradation (same initial CBZ concentration) was observed after 300 min sunlight/H₂O₂ (20 mg L⁻¹) treatment ($Q_{UV} = 19.3 \text{ kJ L}^{-1}$) in WW (Ferro et al., 2015). When UV-C radiation was used as light source in UV-C/PAA process, an higher efficiency was observed (77% removal, $Q_{UV} = 71.78 \text{ kJ L}^{-1}$), but the removal efficiency (22%) observed for 1 mg PAA L⁻¹ is not consistent with previous work (90% removal within 30 min, CBZ initial concentration 1 μM) (Cai et al., 2017). Unlike of CBZ, high removal efficiencies were observed for DCF and SMX in sunlight/PAA experiments, with significantly improved removals in UV-C/PAA tests. However, DCF degradation was drastically affected by aqueous matrix, with a remarkable decreased efficiency in WW (Fig. 5b) compared to GW (Fig. 4b), in particular at lower PAA concentrations. These results can be explained by the higher oxidant demand of WW compared to GW (confirmed by the PAA and H₂O₂ consumption for tests with low concentrations of PAA, Figures SI2 and SI3). Water matrix effect was also observed for SMX degradation by sunlight/PAA and its removal is consistent with previous works with other solar driven AOPs. As matter of fact, Karaolia et al. (2017) observed complete removal of SMX (initial spiked concentration 100 $\mu\text{g L}^{-1}$) by solar photo-Fenton in urban wastewater in a CPC reactor (50 mg H₂O₂ L⁻¹ and 5 mg Fe²⁺ L⁻¹, 119 min of normalized irradiation time ($t_{30W,n}$)).

Interestingly, similar removal trends were observed for DCF and SMX in sunlight/PAA experiments, in both water matrices investigated. The removal efficiency first increased as initial PAA was increased, then started to decrease. Possibly, the reduced efficiency may be due to the scavenging effect of PAA on HO[•] because of the higher PAA concentration (Cai et al., 2017).

5. Conclusions

Photo-driven AOP with PAA was investigated as possible tertiary treatment method of urban wastewater by evaluating its efficiency in the inactivation of AR *E. coli* and degradation of a mixture of three CECs under different light sources. Low PAA doses were found to be effective in the inactivation of AR *E. coli*, being UV-C driven process faster (LOD achieved at $Q_{UV} = 0.3 \text{ kJ L}^{-1}$ with 0.2 mg PAA L⁻¹) than solar driven one (LOD achieved at $Q_{UV} = 4.4 \text{ kJ L}^{-1}$ with 0.2 mg PAA L⁻¹). Higher Q_{UV} and PAA initial doses are necessary to effectively remove the target CECs (being CBZ the more refractory) and, although process efficiency in sunlight tests is lower compared to UV-C radiation, sunlight driven process is still an interesting option for small wastewater treatment plants taking into account that CECs occur at low concentrations (typically in the range ng L⁻¹ - fractions of $\mu\text{g L}^{-1}$). However, initial PAA dose should be optimized to find the best compromise between target bacteria inactivation and CECs removal as well as to prevent scavenging effect of PAA on HO[•] because of high PAA concentration.

Declaration of interests

The authors declare that they have no known competing financial interests or personal relationships that could have appeared to influence the work reported in this paper.

The authors declare the following financial interests/personal relationships which may be considered as potential competing interests.

Acknowledgements

The authors wish to thank European Commission for supporting Teresa Agovino's visit at Plataforma Solar de Almeria in the context of ERASMUS programme.

Appendix A. Supplementary data

Supplementary data to this article can be found online at <https://doi.org/10.1016/j.watres.2018.11.031>.

References

- Ahmed, M.J., 2017. Adsorption of quinolone, tetracycline, and penicillin antibiotics from aqueous solution using activated carbons: Review. *Environ. Toxicol. Pharmacol.* 50, 1–10.
- Antonelli, M., Rossi, S., Mezzanotte, V., Nurizzo, C., 2006. Secondary effluent disinfection: PAA long term efficiency. *Environ. Sci. Technol.* 40, 4771–4775.
- Antonelli, M., Turolla, A., Mezzanotte, V., Nurizzo, C., 2013. Peracetic acid for secondary effluent disinfection: a comprehensive performance assessment. *Water Sci. Technol.* 68 (12), 2638–2644.
- Bourgin, M., Beck, B., Boehler, M., Borowska, E., Fleiner, J., Salhi, E., Teichler, R., von Gunten, U., Siegrist, H., McArdell, C.S., 2018. Evaluation of a full-scale wastewater treatment plant upgraded with ozonation and biological post-treatments: abatement of micropollutants, formation of transformation products and oxidation by-products. *Water Res.* 129, 486–498.
- Brack, W., Dulio, V., Ågerstrand, M., Allan, I., Altenburger, R., Brinkmann, M., Bunke, D., Burgess, R.M., Cousins, I., Escher, B.I., Hernández, F.J., Hewitt, L.M., Hilscherová, K., Hollender, J., Hollert, H., Kase, R., Klauer, B., Lindim, C., López Herráez, D., Miège, C., Munthe, J., O'Toole, S., Posthuma, L., Rüdél, H., Schäfer, R.B., Sengl, M., Smedes, F., van de Meent, D., van den Brink, P.J., van Gils, J., van Wezel, A.P., Vethaak, A.D., Vermeirssen, E., von der Ohe, P.C., Vrana, B., 2017. Towards the review of the European Union Water Framework management of chemical contamination in European surface water resources. *Sci. Total Environ.* 576, 720–737.
- Cai, M., Sun, P., Zhang, L., Huang, C.-H., 2017. UV/Peracetic acid for degradation of pharmaceuticals and reactive species evaluation. *Environ. Sci. Technol.* 51, 14217–14224.
- Calisto, V., Rosário Domingues, M., Erny, G.L., Esteves, V.I., 2011. Direct photodegradation of carbamazepine followed by micellar electrokinetic chromatography and mass spectrometry. *Water Res.* 45, 1095–1104.
- Caretti, C., Lubello, C., 2003. Wastewater disinfection with PAA and UV combined treatment: a pilot plant study. *Water Res.* 37, 2365–2371.
- Cho, M., Chung, H., Choi, W., Yoon, J., 2004. Linear correlation between inactivation of *E. coli* and OH radical concentration in TiO₂ photocatalytic disinfection. *Water Res.* 38, 1069–1077.
- De Souza, J.B., Queiroz Valdez, F., Jeranoski, R.F., de Sousa Vidal, C.M., Soares Cavallini, G., 2015. Water and wastewater disinfection with peracetic acid and UV radiation and using advanced oxidative process PAA/UV. *Int. J. Photoenergy* 1–7. Article ID 860845. <https://doi.org/10.1155/2015/860845>.
- Fatta-Kassinos, D., Manaia, C., Berendonk, T.U., Cytryn, E., Bayona, J., Chefetz, B., Slobodnik, J., Kreuzinger, N., Rizzo, L., Malato, S., Lundy, L., Ledin, A., 2015. COST Action ES1403: new and Emerging challenges and opportunities in wastewater REUSE (NEREUS). *Environ. Sci. Pollut. Res.* 22, 7183–7186.
- Ferro, G., Polo-López, M.I., Martínez-Piernas, A.B., Fernández-Ibáñez, P., Agüera, A., Rizzo, L., 2015. Cross-Contamination of residual emerging contaminants and antibiotic resistant bacteria in lettuce crops and soil irrigated with wastewater treated by sunlight/H₂O₂. *Environ. Sci. Technol.* 49, 11096–11104.
- Fiorentino, A., Ferro, G., Castro, A.M., Polo-López, M.I., Fernández-Ibáñez, P., Rizzo, L., 2015. Inactivation and regrowth of multidrug resistant bacteria in urban wastewater after disinfection by solar-driven and chlorination processes. *J. Photochem. Photobiol. B Biol.* 148, 43–50.
- Formisano, F., Fiorentino, A., Rizzo, L., Carotenuto, M., Pucci, L., Giugni, M., Lofrano, G., 2016. Inactivation of *Escherichia coli* and *Enterococci* in urban wastewater by sunlight/PAA and sunlight/H₂O₂ processes. *Process Saf. Environ. Protect.* 104, 178–184.
- Foster, H.A., Ditta, I.B., Varghese, S., Steele, A., 2011. Photocatalytic disinfection using titanium dioxide: spectrum and mechanism of antimicrobial activity. *Appl. Microbiol. Biotechnol.* 90, 1847–1868.
- Fu, W., Li, B., Yan, J., Y. H., Liyuan, C., Li, X., 2018. New insights into the chlorination of sulfonamide: smiles-type rearrangement, desulfation, and product toxicity. *Chem. Eng. J.* 331, 785–793.
- HACH, 2014. Determination of Peracetic Acid and Hydrogen Peroxide in Water. Application Note.
- Hollender, J., Zimmermann, S.G., Koepke, S., Krauss, M., McArdell, C.S., Ort, C., Singer, H., von Gunten, U., Hansruedi, S., 2009. Elimination of organic micropollutants in a municipal wastewater treatment plant upgraded with a full-scale post-ozonation followed by sand filtration. *Environ. Sci. Technol.* 43, 7862–7869.
- Huang, H., Wu, Q.-Y., Tang, X., Jiang, R., Hu, H.-Y., 2016. Formation of haloacetonitriles and haloacetamides and their precursors during chlorination of secondary effluents. *Chemosphere* 144, 297–303.
- ISO 16075, 2015. Guidelines for Treated Wastewater Use for Irrigation Projects. International Organization for Standardization, Geneva, Switzerland.
- JRC (Joint Research Centre), 2015. Development of the First Watch List under the Environmental Quality Standards Directive: Directive 2008/105/EC, as Amended by Directive 2013/39/EU, in the Field of Water Policy. Raquel N. Carvalho, Lidia Ceriani, Alessio Ippolito and Teresa Lettieri. Report EUR 27142 EN.
- Karaolia, P., Michael-Kordatou, I., Hapeshi, E., Alexander, J., Schwartz, T., Fatta-

- Kassinis, D., 2017. Investigation of the potential of a Membrane BioReactor followed by solar Fenton oxidation to remove antibiotic-related micro-contaminants. *Chem. Eng. J.* 310, 491–502.
- Keun-Young, P., Su-Young, C., Seung-Hoon, L., Ji-Hyang, K., Ji-Hyeon, S., 2016. Comparison of formation of disinfection by-products by chlorination and ozonation of wastewater effluents and their toxicity to *Daphnia magna*. *Environ. Pollut.* 215, 314–321.
- Klamerth, N., Rizzo, L., Malato, S., Maldonado, M.I., Agüera, A., Fernández-Alba, A.R., 2010. Degradation of fifteen emerging contaminants at $\mu\text{g L}^{-1}$ initial concentrations by mild solar photo-Fenton in MWTP effluents. *Water Res.* 44, 545–554.
- Koivunen, J., Heinonen-Tanski, H., 2005. Inactivation of enteric microorganisms with chemical disinfectants, UV irradiation and combined chemical/UV treatments. *Water Res.* 39, 1519–1526.
- Kowalski, W., 2009. *Ultraviolet Germicidal Irradiation Handbook*. Springer-Verlag Berlin Heidelberg. https://doi.org/10.1007/978-3-642-01999-9_2.
- Krzeminski, P., Tomei, M.C., Karaolia, P., Langenhoff, A., Almeida, C.M.A., Felis, E., Gritten, F., Andersen, H.R., Fernandes, T., Manaia, C.M., Rizzo, L., Fatta-Kassinis, D., 2019. Performance of secondary wastewater treatment methods for the removal of contaminants of emerging concern implicated in crop uptake and antibiotic resistance spread: a review. *Sci. Total Environ.* 648, 1052–1081.
- Lian, J., Qiang, Z., Li, M., Bolton, J.R., Qu, J., 2015. UV photolysis kinetics of sulfonamides in aqueous solution based on optimized fluence quantification. *Water Res.* 75, 43–50.
- Lubello, C., Caretti, C., Gori, R., 2002. Comparison between PAA/UV and H₂O₂/UV disinfection for wastewater reuse. *Water Science and Technology. Water Supply* 2 (1), 205–212.
- Malato, S., Fernandez-Ibanez, P., Maldonado, M.I., Blanco, J., Gernjak, W., 2009. Decontamination and disinfection of water by solar photocatalysis: recent overview and trends. *Catal. Today* 147, 1–59.
- Martin, N., Gehr, R., 2007. Reduction of photoreactivation with the combined UV/peracetic acid process or by delayed exposure to visible light. *Water Environ. Res.* 79, 991–999.
- McGuigan, K.G., Conroy, R.M., Mosler, H.-J., du Preez, M., Ubomba-Jaswa, E., Fernandez-Ibanez, P., 2012. Solar water disinfection (SODIS): a review from bench-top to roof-top. *J. Hazard Mater.* 235–236, 29–46.
- Petrie, B., Barden, R., Kasprzyk-Hordern, B., 2015. A review on emerging contaminants in wastewaters and the environment: current knowledge, understudied areas and recommendations for future monitoring. *Water Res.* 72, 3–27.
- Polo-López, M.I., Fernández-Ibáñez, P., García-Fernández, I., Oller, I., Salgado-Tránsito, I., Sichel, C., 2010. Resistance of *Fusarium* sp spores to solar TiO₂ photocatalysis: influence of spore type and water (scaling-up results). *J. Chem. Technol. Biotechnol.* 85, 1038–1048.
- Rizzo, L., Della Sala, A., Fiorentino, A., Li Puma, G., 2014. Disinfection of urban wastewater by solar driven and UV lamp – TiO₂ photocatalysis: effect on a multi drug resistant *Escherichia coli* strain. *Water Res.* 53, 145–152.
- Rizzo, L., Fiorentino, A., Anselmo, A., 2012. Effect of solar radiation on multidrug resistant *E. coli* strains and antibiotic mixture photodegradation in wastewater polluted stream. *Sci. Total Environ.* 427–428, 263–268.
- Rizzo, L., Fiorentino, A., Grassi, M., Attanasio, D., Guida, M., 2015. Advanced treatment of urban wastewater by sand filtration and graphene adsorption for wastewater reuse: effect on a mixture of pharmaceuticals and toxicity. *Journal of Environmental Chemical Engineering* 3, 122–128.
- Rizzo, L., Kraetke, R., Linders, J., Scott, M., Vighi, M., de Voogt, P., 2018. Proposed EU minimum quality requirements for water reuse in agricultural irrigation and aquifer recharge: SCHEER scientific advice. *Current Opinion in Environmental Science & Health* 2, 7–11.
- Rizzo, L., Manaia, C.M., Merlin, C., Schwartz, T., Dagot, C., Ploy, M.C., Michael, I., Fatta-Kassinis, D., 2013. Urban wastewater treatment plants as hotspots for antibiotic resistant bacteria and genes spread into the environment: a review. *Sci. Total Environ.* 447, 345–360.
- Sacco, O., Vaiano, V., Rizzo, L., Sannino, D., 2018. Photocatalytic activity of a visible light active structured photocatalyst developed for municipal wastewater treatment. *J. Clean. Prod.* 175, 38–49.
- Trovó, A.G., Nogueira, R.F.P., Agüera, A., Sirtori, C., Fernández-Alba, A.R., 2009. Photodegradation of sulfamethoxazole in various aqueous media: persistence, toxicity and photoproducts assessment. *Chemosphere* 77, 1292–1298.
- USEPA, 2012. *Guidelines for Water Reuse*. United States Environmental Protection Agency, Washington, DC, USA (EPA/600/R-12/618).
- Yuan, Q., Guo, M., Yang, J., 2015. Fate of antibiotic resistant bacteria and genes during wastewater chlorination: implication for antibiotic resistance control. *PLoS One* 10 (3), e0119403.
- Zhang, C., Brown, P.J.B., Hu, Z., 2018. Thermodynamic properties of an emerging chemical disinfectant, peracetic acid. *Sci. Total Environ.* 621, 948–959.
- Zhang, N., Liu, G., Liu, H., Wang, Y., He, Z., Wang, G., 2011. Diclofenac photodegradation under simulated sunlight: effect of different forms of nitrogen and Kinetics. *J. Hazard Mater.* 192, 411–418.